Int J. Heat Mass Transfer. Vol 21, pp 1619–1621
Pergamon Press Ltd. 1978. Printed in Great Britain

SHORTER COMMUNICATIONS

FINITE ELEMENT ANALYSIS OF COMBINED FREE AND FORCED CONVECTION

S. DEL GIUDICE,* G. COMINI† and M. D. MIKHAILOV‡

NOMENCLATURE

A,	cross-sectional area, dimensionless;§
L,	pressure gradient parameter, dimensionless;
l_x, l_y,	direction cosines of the outward normal;
n,	outward normal;
Nu,	Nusselt number, dimensionless;
R, I,	variables defined by equation (5), dimensionless;
Ra,	Rayleigh number, dimensionless;
t,	dimensionless temperature;
w,	dimensionless axial velocity;
x, y,	dimensionless coordinates.

Subscripts

m,	average value;
x, y,	in the x, y direction.

INTRODUCTION

RECENTLY, in the study of heat conduction with periodic boundary conditions, the authors used a complex function whose real and imaginary components are related to the amplitude and phase angle of temperature oscillations [1]. The resulting homogeneous wave equation in complex domain was treated as a system of two equations in which all quantities are real. Parabolic elements and the Galerkin weighted residual process were used in the finite element solution.

Since several heat-transfer processes can be described in terms of a Helmoltz wave equation in complex domain, the computer code developed in [1] has other utilizations besides the solution of periodic heat-conduction problems.

In this note the technique proposed in [1] is applied to the analysis of combined free and forced convection in a fully developed laminar steady flow through vertical ducts, with arbitrary cross-sections, under the conditions of constant axial heat flux and uniform peripheral wall temperatures.

In the context of the finite element method, a similar problem has been dealt with by Nayak and Cheng [2], using triangular elements and piecewise linear polynomials for the interpolation of temperature and velocity profiles. However, their finite element formulation presents severe disadvantages, such as the use of the pressure gradient value L as an input datum and, apparently, the inability to allow for natural (i.e. zero flux) boundary conditions.

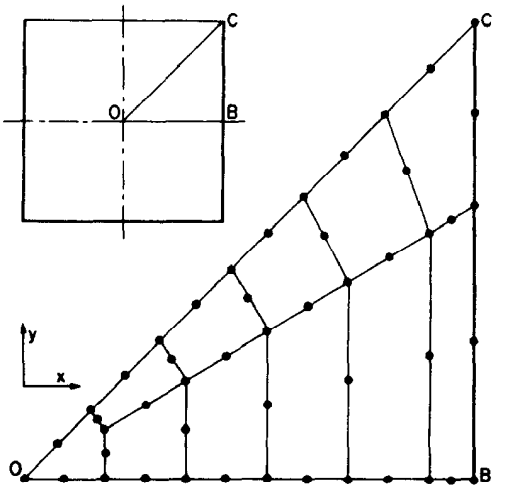

FIG. 1. Finite element mesh used for the analysis of a square geometry. Because of existing symmetry only a right angled isosceles sector is considered and natural (i.e. zero flux) boundary conditions on OC and OB are assumed. Uniform temperatures and zero velocities are assumed on BC.

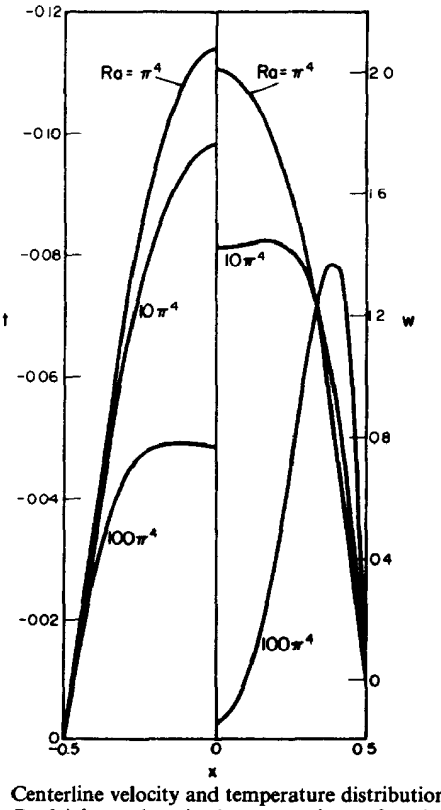

FIG. 2. Centerline velocity and temperature distributions at various Rayleigh numbers in the square duct referred to in Fig. 1.

*Istituto di Fisica Tecnica dell'Università, via Marzolo 9, 35100 Padova, Italy, and Laboratorio per la Tecnica del Freddo del C.N.R., Cas. Post. 1075, 35100 Padova, Italy.

†Istituto di Fisica Tecnica dell'Università, via Valerio 10, 34127 Trieste, Italy, and Laboratorio per la Tecnica del Freddo del C.N.R.

‡Applied Mathematics Centre, VMEI, P.O.B. 384, Sofia C, Bulgaria.

§Standard definitions are used for dimensionless quantities (see for example [2, 3, 5]).

Table 1. Comparison between analytical (AN) and finite element (FEM) solutions for a square duct at various Rayleigh numbers

Ra	Nu		L	
	AN [3]	FEM	AN [3]	FEM
100	3.70	3.70	35.26	35.31
1000	4.47	4.45	90.35	90.58
10000	8.40	8.32	429.8	432.7

MATHEMATICAL FORMULATION

The problem is described in [2] by the system of equations:

$$\left.\begin{aligned} \frac{\partial^2 t}{\partial x^2}+\frac{\partial^2 t}{\partial y^2}-w=0 \\ \frac{\partial^2 w}{\partial x^2}+\frac{\partial^2 w}{\partial y^2}-Rat+L=0 \end{aligned}\right\} \quad (1)$$

where t and w are dimensionless temperature and velocity respectively, x and y are dimensionless coordinates, L is the pressure gradient parameter and Ra is the Rayleigh number.

Boundary conditions are:

$$t=w=0 \quad (2)$$

on part of the boundary Γ_1 and

$$\frac{\partial t}{\partial x}l_x+\frac{\partial t}{\partial y}l_y=\frac{\partial w}{\partial x}l_x+\frac{\partial w}{\partial y}l_y=0 \quad (3)$$

on part of the boundary Γ_2, (l_x, l_y) being the direction cosines of the outside normal to the boundary surface (as pointed out previously, boundary condition (3) was not considered in [2]).

The average Nusselt number is given by:

$$Nu=-1/4t_m,\quad t_m=\iint wt\,dA/\iint w\,dA \quad (4)$$

when A is the cross-sectional area of the duct.

Table 2. Calculated Nusselt numbers and pressure gradient parameters at various Rayleigh numbers for geometries a and b in Fig 3

Ra	Nu_a	L_a	Nu_b	L_b
100	15.08	82.29	15.27	80 40
1000	15.18	97.16	15.32	95.12
10000	16.03	241 3	15.75	240.0

Let the two variables

$$\left.\begin{aligned} R=\frac{w}{L}-t\frac{Ra^{1/2}}{L}-\frac{1}{Ra^{1/2}}, \\ I=\frac{w}{L}+t-\frac{Ra^{1/2}}{L}+\frac{1}{Ra^{1/2}} \end{aligned}\right\} \quad (5)$$

be introduced. Multiplying the first equation (1) by $Ra^{1/2}$, subtracting and adding the result from the second equation (1) and finally dividing by L leads to the new system of equations:

$$\left.\begin{aligned} \frac{\partial^2 R}{\partial x^2}+\frac{\partial^2 R}{\partial y^2}+Ra^{1/2}I=0 \\ \frac{\partial^2 I}{\partial x^2}+\frac{\partial^2 I}{\partial y^2}-Ra^{1/2}R=0. \end{aligned}\right\} \quad (6)$$

Boundary conditions with the new variables are:

$$R=-1/Ra^{1/2},\quad I=1/Ra^{1/2} \text{ on } \Gamma_1 \quad (2')$$

and

$$\frac{\partial R}{\partial n}=\frac{\partial I}{\partial n}=0 \text{ on } \Gamma_2. \quad (3')$$

The computer program described in [1] was developed for the problem:

$$\left.\begin{aligned} \frac{\partial}{\partial x}\left(k_x\frac{\partial R}{\partial x}\right)+\frac{\partial}{\partial y}\left(k_y\frac{\partial R}{\partial y}\right)+\omega\rho cI=0 \\ \frac{\partial}{\partial x}\left(k_x\frac{\partial I}{\partial x}\right)+\frac{\partial}{\partial y}\left(k_y\frac{\partial I}{\partial y}\right)-\omega\rho cR=0 \end{aligned}\right\} \quad (7)$$

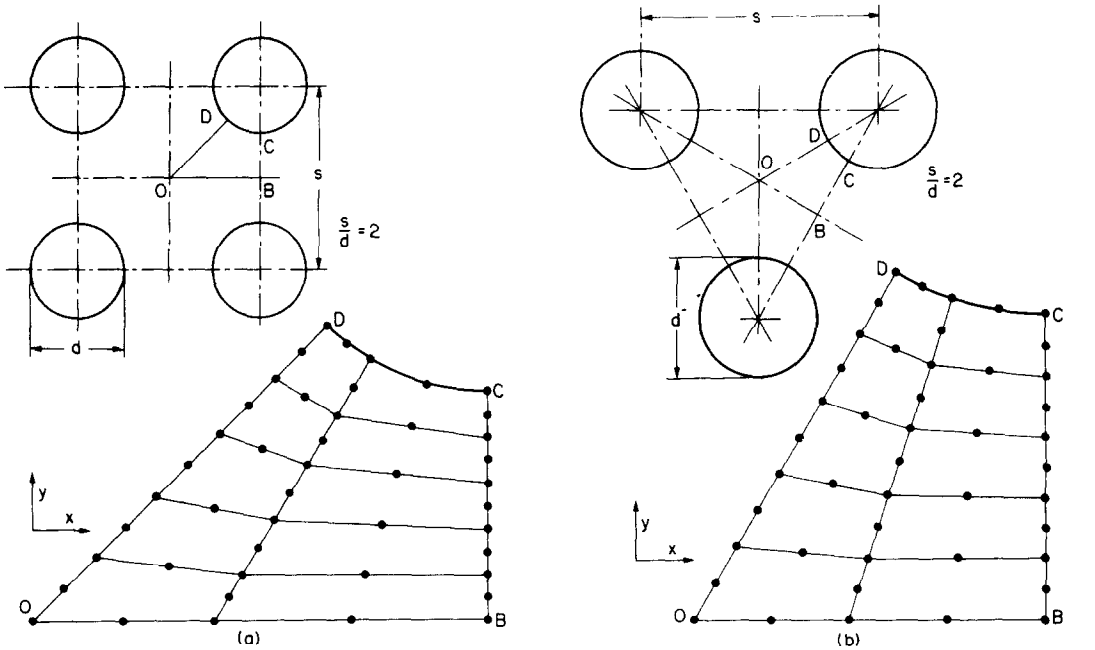

FIG. 3. Finite element meshes used in the analysis of two realistic problems. The existing symmetries are fully exploited by assuming natural (i.e. zero flux) boundary conditions where appropriate. Again uniform temperatures and zero velocities are assumed on tube walls.

subjected to boundary conditions:

$$R = R_w, \quad I = I_w \quad \text{on} \quad \Gamma_1 \tag{8}$$

and

$$\left.\begin{aligned} k_x \frac{\partial R}{\partial x} l_x + k_y \frac{\partial R}{\partial y} l_y &= q_R, \\ k_x \frac{\partial I}{\partial x} l_x + k_y \frac{\partial I}{\partial y} l_y &= q_I \end{aligned}\right\} \text{on} \quad \Gamma_2. \tag{9}$$

Therefore, problem (6), (2'), (3') is a special case of problem (7)–(9). Consequently the computer code described in [1] can be used, without modifications, for the analysis of combined free and forced convection in a fully developed laminar steady flow.

After the values of R and I are obtained, dimensionless temperature and velocity distributions can be computed from the formulae:

$$w = \frac{R+I}{2} L, \quad t = \left[\frac{I-R}{2(Ra)^{1/2}} - \frac{1}{Ra}\right] L \tag{10}$$

where [3–5]:

$$L = \iint \mathrm{d}A / \iint (w/L)\,\mathrm{d}A. \tag{11}$$

EXAMPLES OF APPLICATION

To assess the accuracy of the finite element code used, computations were carried out for a square duct. The geometry considered and the finite element mesh utilized are shown in Fig. 1. Because of the existing symmetry, the analysis is limited to a right-angled isosceles sector and natural (i.e. zero flux) boundary conditions are assumed on the internal sides.

In Table 1 numerical results for the Nusselt number Nu and the pressure gradient parameter L are compared with analytical solution [3]. As it can be seen, isoparametric elements yield a good agreement even if a relatively coarse mesh is used.

Temperature and velocity distribution over the square centerline are shown in Fig. 2. The results compare favourably with the most accurate calculations in [2], where a much larger number of nodal points was used.

To demonstrate the capabilities of the program in dealing with complex realistic problems, velocity and temperature distributions were computed for the geometries shown in Fig. 3. The resulting values of the Nusselt number Nu and of the pressure gradient parameter L for the two geometrical situations are reported in Table 2 as a function of the Rayleigh number.

REFERENCES

1. M. D. Mikhailov, G. Comini, S. Del Giudice and G. P. Runchi, Determination of thermal wave distributions by the finite element method, *Int. J. Heat Mass Transfer* **20**, 195–200 (1977).
2. A. L. Nayak and P. Cheng, Finite element analysis of laminar convective heat transfer in vertical ducts with arbitrary cross-sections, *Int. J. Heat Mass Transfer* **18**, 227–236 (1975).
3. M. Iqbal, S. A. Ansari and B. D. Aggarwala, Effect of buoyancy on forced convection in vertical regular polygonal ducts, *J. Heat Transfer* **92**, 237–244 (1970).
4. L. S. Han, Laminar heat transfer in rectangular channels, *J. Heat Transfer* **81**, 121–128 (1959).
5. M. Iqbal, B. D. Aggarwala and A. G. Fowler, Laminar combined free and forced convection in vertical non-circular ducts under uniform heat flux, *Int. J. Heat Mass Transfer* **12**, 1123–1139 (1969).

Int J. Heat Mass Transfer Vol. 21, pp. 1621–1624

0017-9310/78/1201-1621 $02.00/0

MEASUREMENT OF TRANSITION BOILING BOUNDARIES IN FORCED CONVECTIVE FLOW

H. S. RAGHEB and S. C. CHENG
Department of Mechanical Engineering, University of Ottawa, Ottawa, Ontario, Canada

and

D. C. GROENEVELD
Chalk River Nuclear Laboratories, Atomic Energy of Canada Limited, Chalk River, Canada

(*Received* 26 *January* 1978 *and in revised form* 8 *May* 1978)

INTRODUCTION

THE TRANSITION boiling heat-transfer mode may be viewed as a combination of unstable (vapor) film boiling and unstable nucleate boiling alternatively existing at any given location on a heated surface. The variation of heat-transfer rate with temperature is primarily a result of the change in the fraction of time that each boiling mode exists at a given location.

The transition boiling mode is most efficient at the boiling crisis point which represents its lower temperature boundary. Conditions here may be predicted by a variety of correlations. The higher temperature boundary of the transition boiling mode takes place at or near the minimum heat flux point where a change from transition boiling to pure film boiling takes place. Little is known about the boundary between transition boiling and film boiling except that it is influenced by flow conditions, fluid properties and surface properties [1, 2].

Knowledge of the temperature boundaries of the transition boiling mode is important in the prediction of the temperature–time history of a hot surface during quenching (e.g. during emergency core cooling of a nuclear reactor). The purpose of this investigation was to determine whether during the quenching process (1) the minimum heat flux corresponds to the initiation of liquid contact on a surface, and (2) whether the critical heat flux corresponds to the initiation of continuous liquid contact [3].

This study is believed to be novel in two ways (a) to the authors' knowledge, no other investigator has ever measured the boundary between film boiling and transition boiling under forced convective conditions, and (b) the probe design is uniquely suited to high temperature operation. Few relevant studies have been reported in the literature. Iida and Kobayasi [4] measured the variation of